dependence of AAE can be used to provide a quantitative estimate of BrC (Sandradewi et al., 2008; Harrison et al., 2012), and also for further distinction of sources (Ajtai et al., 2011; Pintér et al., 2018). However, theoretical calculations and field studies have shown that the likely range of AAE for internally mixed BC varies in a range of approximate 1-1.7, depending on the size and optical properties of the particle core and non-absorbing coating and the wavelength pairs used to determine AAE (Gyawali et al., 2009; Lack and Cappa, 2010; Lin et al., 2016). Using a three wavelength photo-acoustic soot spectrometer (PASS-3) and aerosol mass spectrometers (AMS), Yuan et al. (2016) explored the relationship between the measured AAE and the relative abundance of organic aerosol to BC and derived more realistic AAE values for "pure" BC aerosol, which is significantly lower than 1. Contributions to total light absorption at 370 nm by BrC were also estimated by comparing the wavelength dependence of the absorption coefficients of aerosols before and after heated (Guo et al., 2014). This is based on the assumption that the change of AAE for aerosols after heated is due to the evaporation of BrC, but the potential error of which has not been fully assessed.

In the present work, the optical, physical, and chemical properties of atmospheric aerosols were measured before and after heated in the Pearl River Delta (PRD) region, China. In this region, organics are the second largest contributor for light extinction (Zhang et al., 2013a; Chen et al., 2016), and the average light absorption contributions of BrC at 405 nm were quantified to be ~10%. This work presents spectral measurements of light absorption coefficient (σ_{abs}) in a broad spectral range (370–950 nm) by an Aethalometer, highlighting some characteristics of light-absorbing aerosols. An improved method was developed, based on wavelength segregated AAE, in order to estimate of the contribution of BrC to light absorption at 370 nm ($\sigma_{abs,BrC}/\sigma_{abs,370nm}$). Meanwhile, the BrC contribution was also compared to those estimated based on the previously reported methods.

2 Methods

2.1 Ambient observation

Ambient measurements were performed at Guangdong Atmospheric Supersite (22.73N, 112.93E), a suburban site (Zhang et al., 2014) in the PRD region from July 8 to August 2, 2014. Over the sampling period, ambient temperature and relative humidity generally varied between 24–37 °C and 40–93%, with an average of 29 °C and 73%, respectively. The concentration of $PM_{2.5}$ varied in a wide range of 0.78–166 μg m^{-3}, with mean value of 29.7 μg m^{-3}. Wind speed ranged between 0.3–5.1 m s^{-1} and the prevailing direction was from southwestern. Wind speed was lower (~1 m s^{-1}) during the early morning hours and was relatively higher (~2 m s^{-1}) in the afternoon.

To compare the properties of aerosols before and after heated, an automatic-controlled actuated ball valve that switches between "bypass" and "heating" on a 5-min cycle. The thermodenuder (TD, Dekati Ltd.) consists of a 95-cm long stainless steel tube, where the particles can be heated with controlled temperature, i.e., 250 ^{o}C. The residence time of particles in the TD section is estimated to be 1.2 s, which should be enough for the effective vaporization of semi-volatile species (Villani et al., 2007). Volatile or semi-volatile species, such as most of organic compounds and ammonium nitrate, are supposed to evaporate during the heating (Bi et al., 2015). Subsequently, these species were adsorbed in active charcoal in the adsorber section. The bypass consists of a silica tube of similar length for heating condition. In order to eliminate the influence of resident aerosols in the tubes, only the measurements during the latter 3-min of the 5-min cycle were included in the following data analysis. Particle loss could be typically represented as a function of flow rate and particle size (Stevanovic et al., 2015). The test made by the manufacturer shows that particles with a physical diameter d_p <= 70 nm have a size dependent particle loss, increasing from ~20% to ~40% when d_p decreases from 70 nm to 10 nm; particle loss at d_p > 70 nm is estimated to be approximately 20% at the total flow rate of 10 lpm, mainly attributed to the diffusion of particles. Regarding that the d_p of refractory BC was reported to be around 200 nm in the PRD region (Huang et al., 2011), the particle loss might lead to a 20% negative bias for σ_{abs} measured through the heated line. The BC around 200 nm was most probably attributed to be from traffic emission, with their diurnal variation similar to that of NO_x (Qin et al., 2017), as shown in Fig. S1.

The σ_{abs} was determined in 1-min resolution by an Aethalometer (AE-33, Magee Scientific) with seven wavelengths (at 370, 470, 520, 590, 660, 880 and 950 nm, respectively). A single particle aerosol mass spectrometer (SPAMS, Hexin Analytical Instrument Co., Ltd.) was deployed to measure the size and mass spectra of individual particles (Li et al., 2011). Aethalometer and SPAMS shared an aerosol inlet (dried total suspended aerosols) and were placed downstream of the TD. Additionally, the concentrations of water soluble ions associated with $PM_{2.5}$ were obtained from a Monitor for AeRosols and GAses in ambient air (MARGA) (Rumsey et al., 2014). Hourly variations of organic carbon (OC)/elemental carbon

(EC) in $PM_{2.5}$ were provided by a Sunset Semi-Continuous Aerosol Analyzer. Concentration of O_3 was measured using an ozone analyzer (Model *49i*, Thermo-Fisher Scientific). For comparison, all the measured parameters were present as hourly averages in this paper. A detailed description of the instruments and the data analysis can be found in Supporting Information (SI).

2.2 Light absorption measurements

Generally, filter-based optical measurement instruments (e.g., Aethalometer) must take into account the "filter loading effect" to accurately determine the σ_{abs} (Arnott et al., 2005; Ajtai et al., 2011). The new version Aethalometer (AE-33) used in the present study has been improved with the filter loading correction part, based on a two parallel spot measurement of optical absorption, through providing a real-time output of the 'loading compensation' parameter to compensate for the "loading effect", in detail described in the SI. The details of operation principle, data deduction, error budget of AE-33, inherent uncertainties in its technique and the corrections are extensively available in the literature (Drinovec et al., 2015). The BC mass concentration is calculated from the change in optical attenuation at 880 nm in the selected time interval using the mass absorption cross section (MAC) of 7.77 $m^2\ g^{-1}$, which is close to that reported in the PRD region (Cheng et al., 2011). The noise level of AE-33 at the time-base of 1 minute is < 0.016 Mm^{-1} for the σ_{abs} (http://www.magescientific.com/). The contribution of dust to σ_{abs} can be considered to be negligible in the PRD region (Yuan et al., 2016), due to limited mass fraction (Cheng et al., 2008; Zhang et al., 2013a), and lower mass absorption efficiency values (Favez et al., 2009).

3 Results and Discussion

3.1 Previous methods to estimate the light absorption from BrC

3.1.1 Method I: assuming AAE = 1 for "pure" BC

The wavelength (λ) dependence of σ_{abs} is usually approximated by a power-law expression (e.g., Bergstrom et al., 2007), defined as:

$$\sigma_{abs} = K \times \lambda^{-AAE} \qquad \text{(R1)}$$

where K is a constant. In practice for multi-wavelength measurements, AAE can be retrieved by fitting the σ_{abs} to the λ (370–950 nm), or to the different wavelength ranges (Bergstrom et al., 2007). Thus, a wavelength segregated AAE value can be obtained through the logarithmic fit of R1, or AAE = $\ln(\sigma_{abs1}/\sigma_{abs2})/\ln(\lambda_1/\lambda_2)$ for two wavelengths.

The AAE has often been used as a simplified method for attributing short visible wavelength absorption to BrC (Lack and Cappa, 2010). Light absorption at longer wavelength (950 nm) is assumed to be due only to BC, and is extrapolated to the shorter wavelength using an assumed AAE, most commonly to be one, which is illustrated in Fig. 1. It estimates the $\sigma_{abs,BrC}$ at 370 nm by subtracting the measured σ_{abs} to the extrapolated $\sigma_{abs,BC}$ at 370 nm ("Method I"):

$$\sigma_{abs,BrC} = \sigma_{abs,370nm} - \sigma_{abs,950nm} \times (370/950)^{-AAE} \qquad \text{(R2)}$$

3.1.2 Method II: based on light absorption enhancement

The $\sigma_{abs,BrC}/\sigma_{abs,370nm}$ was also estimated based on the enhancements of σ_{abs} (E_{abs}), defined as the ratio of σ_{abs} for ambient and heated aerosols ($E_{abs} = \sigma_{abs,ambient}/\sigma_{abs,TD}$), at both 370 and 950 nm in previous studies (Cappa et al., 2012; Guo et al., 2014).

$$\sigma_{abs,BrC}/\sigma_{abs,370nm} = (E_{abs,370nm} - E_{abs,950nm})/E_{abs,370nm} \quad \text{(R3)}$$

where $\sigma_{abs,BrC}$ refers to the effective absorption coefficient at 370 nm for the BrC evaporating under the TD temperature (i.e., 250 ^{o}C), which is slightly different from the definition in R2. When there is no evaporative BrC, $E_{abs,950nm}$ should equal to $E_{abs,370nm}$, since evaporation of BrC would result in larger $E_{abs,370nm}$ than $E_{abs,950nm}$ (Cappa et al., 2012). It is worthy to note that this estimation (R3) actually represents the net result of evaporation and production of BrC in measured aerosol fraction.

3.2 An improved AAE-based method developed by this study

As far as the wavelength segregated AAE is concerned (Sandradewi et al., 2008; Mogo et al., 2012; Utry et al., 2014), the AAE determined over the wavelength of 370–520 nm and 880–950 nm and their diurnal variations were compared in Fig. 2. $AAE_{370\text{-}520}$ were 1.36 ± 0.25 and 1.41 ± 0.22, and $AAE_{880\text{-}950}$ were 0.70 ± 0.07 and 0.68 ± 0.08 for ambient and heated particles, respectively. $AAE_{880\text{-}950}$ were quite similar, indicating there was a thin coating and negligible lensing effect, which could be supported by the chemical composition of the ambient and heated BC-containing particles detected by the SPAMS (Fig. S2). It can be seen that $AAE_{880\text{-}950}$ varied in a narrow range (0.63–0.78, 10^{th}–90^{th} of the observed data), and significant difference

(p < 0.001) was found between $AAE_{370-520}$ and $AAE_{880-950}$ for both ambient and heated particles, respectively. It reflects that σ_{abs} becomes more sensitive to spectral variations at lower wavelengths than at higher wavelengths, which is attributed to the presence of BrC (Mogo et al., 2012). While AAE is sensitive to these microphysical properties (Moosmüller et al., 2009; Lack and Cappa, 2010), the influence of particle size on the AAE for heated aerosols should be limited in the present study, since the difference of hourly average $AAE_{880-950}$ for aerosols before and after heated was in a small range (2% ± 2%). Furthermore, there is no significant correlation (p > 0.05) between $AAE_{880-950}$ and mass fraction ratio of available coating materials ($PM_{2.5}$-BC) to BC, which further indicates limited influence of coating materials on the $AAE_{880-950}$. In contrast, the difference between $AAE_{370-520}$ for aerosols before and after heated was relatively higher (–5% ± 11%), which is more evidently shown in their diurnal variation (Fig. 2b). Correlation coefficients (r^2) between $AAE_{370-520}$ and $AAE_{590-950}$, $AAE_{660-950}$, and $AAE_{880-950}$ are 0.56, 0.48 and 0.17, respectively, implying limited influence of BrC on the $AAE_{880-950}$. Overall, these results supported that $AAE_{880-950}$ may well represent the AAE of BC dominant aerosols in the present study. "Pure" BC AAE (i.e., $AAE_{880–950}$) of 0.70 ± 0.07 inferred in this study is significantly lower than the widely adopted value (AAE = 1) (Bond and Bergstrom, 2006). While it might not typical to have AAE of the "pure" BC lower than one, the retrieved value in this study is quite similar to that (AAE between the wavelength at 532 and 781 nm) estimated for the "pure" BC dominated from traffic emission in the same region (Yuan et al., 2016). Additionally, lower AAE values (< 1) have also been reported for the "pure" BC in traffic and biomass burning emissions (Kirchstetter et al., 2004), and at urban site in Beijing

(Wu et al., 2015). Theoretical calculation shows that AAE decreases with the increasing of "pure" BC sizes (Wu et al., 2015). Regarding the reported volume equivalent diameter peak of "pure" BC to be around 200 nm in this region (Huang et al., 2011), the corresponding theoretical AAE would most probably vary between 0.4 and 1 (Wu et al., 2015). In addition, the fractal like structure of combustion generated BC could also be one possible explanation of the smaller value of AAE measured in this study (Moosmüller et al., 2009; Lack and Cappa, 2010). Therefore, based on the assumption that BC is the dominant absorbing species over the near-IR wavelength (Shrestha et al., 2014), it is proposed to apply AAE = $AAE_{880\text{-}950}$, instead of AAE = 1, in R2 to estimate $\sigma_{abs,BrC}$. Additionally, the input of hourly variation of $AAE_{880\text{-}950}$ further accounts for the factors (e.g., sources and atmospheric processing) that have influence on $AAE_{880\text{-}950}$ of BC dominant aerosols.

The uncertainty associated with this method was estimated through a sensitivity test. The upper and lower bound of hourly average σ_{abs} (σ_{abs} ± std (σ_{abs}), std (σ_{abs}) refers to the standard deviation of σ_{abs}) were inputted in R1 and R2 to obtain an estimate of the upper and lower bound of $\sigma_{abs,BrC}$. Std (σ_{abs}) at 1 min time base is assumed to be three times the noise level (0.016 Mm^{-1}) of AE33, and thus hourly based std (σ_{abs}), averaged over 18 mins measurements of ambient aerosols could be calculated as: $3 \times \sqrt{18} \times 0.016\ \mathrm{Mm}^{-1} = 0.2\ \mathrm{Mm}^{-1}$. The upper and lower bounds of $\sigma_{abs,BrC}$ was calculated to be 28.8 and 27.1 Mm^{-1} on average, respectively, which is within 3% difference compared to the mean value of $\sigma_{abs,BrC}$ (28.0 Mm^{-1}).

Based on the improved AAE based method, the temporal profiles of the estimated $\sigma_{abs,BrC}$ in Guangdong Atmospheric Supersite as well as the concentration of potassium, the correlation between $\sigma_{abs,BrC}$ and BC concentration, and the frequency histogram of the $\sigma_{abs,BrC}/\sigma_{abs,370nm}$ are shown in Fig. 3. The estimated $\sigma_{abs,BrC}/\sigma_{abs,370nm}$ distributed within a range of 30%–50%, with an average value at 37.4% ± 7.1%. Significant correlation (r^2 = 0.72) between the estimated $\sigma_{abs,BrC}$ and BC demonstrates their similar sources (Andreae and Gelencser, 2006; Moosmüller et al., 2009; Saleh et al., 2013; Guo et al., 2014). The correlation between the estimated $\sigma_{abs,BrC}$ and the concentration of potassium, which is commonly used as a marker for biomass burning activities, was also observed to be significant ($r^2 = 0.38$, $p < 0.001$), indicative of potential contribution of biomass burning to the observed BrC (Lack et al., 2013; Saleh et al., 2014; Hsiao et al., 2016; Rathod et al., 2017) in the PRD region. Potassium originated from sea salt and dust (Pio et al., 2007) was estimated to be < 5% of the observed potassium in our study. Moderate correlation could be partly explained by that emission of BrC from biomass burning is linked to both burning condition and the emitted organic tracers (Lack et al., 2013; Saleh et al., 2014), and also other sources.

3.3 Comparisons of the method developed in this study with the previous methods

3.3.1 Comparison with Method I

It is necessary to note that applying AAE = 1 to anchor absorption for BC and BrC may introduce potential errors, since the AAE for ambient particles (measured between a short and long visible wavelength) has often been observed to be variable, dependent on their physical and chemical properties (Mogo et al., 2012; Lack and Langridge, 2013). Fig. 1 shows the average AAE (1.36 ± 0.25 and 0.70 ± 0.07) of the ambient particles estimated from the linear fit (R1) of σ_{abs} over the wavelength of 370–520 nm and 880–950 nm, respectively.

Based on AAE = 1 assumption, $\sigma_{abs,BrC}/\sigma_{abs,370nm}$ was calculated to be 16.8% ± 11%. While the estimated $\sigma_{abs,BrC}/\sigma_{abs,370nm}$ based on AAE = $AAE_{880\text{-}950}$ (the developed method) and AAE = 1 is highly correlated ($r^2 = 0.78$, $p < 0.001$, Fig. 4), the difference can be as large as 20% on average. There were some negative values obtained when assuming AAE = 1, because the observed $AAE_{370\text{-}950}$ was lower than one during some periods. Therefore, an arbitrary attribution of AAE to be one may substantially underestimate the $\sigma_{abs,BrC}/\sigma_{abs,370nm}$.

3.3.2 Comparison with Method II

Based on the Method II, the average estimated $\sigma_{abs,BrC}/\sigma_{abs,370nm}$ over the study was –2.4% ± 11.5%, which indicates that production of BrC dominated over evaporation, resulted in a net production of BrC when ambient aerosols were heated. Similar estimation in previous studies also resulted in the negative values for $\sigma_{abs,BrC}/\sigma_{abs,370nm}$ (Guo et al., 2014; McMeeking et al., 2014; Nakayama et al., 2014), and it was attributed to the production of BrC when ambient aerosols were heated (Nakayama et al., 2014). A comparison of the $\sigma_{abs,BrC}/\sigma_{abs,370nm}$ estimated by the Methods II and the developed method in Fig. 5 indicates that the production of BrC during heating periods can be substantially important, which may account for > 40% difference between the estimated $\sigma_{abs,BrC}/\sigma_{abs,370nm}$, and thus should be emphasized when estimating $\sigma_{abs,BrC}/\sigma_{abs,370nm}$ with the Method II. The uncertain evaporation state of BrC during heating might be partly explained by the residue chemical information (Fig. S2). The increased difference during afternoon hours (~50%) (Fig. 5) may further indicate the influence of photochemical activity on the production of BrC during the heating periods. This could be evidenced by negative correlations (p < 0.001) between the estimated $\sigma_{abs,BrC}/\sigma_{abs,370nm}$ by Method II and the concentrations of secondary organic carbon (SOC, see SI) and O_3 (Fig. 6). This connection is probably explained by the conversion of SOC to BrC when aerosols were heated, and the conversion should be improved when there are high level of SOC and O_3. Such fraction of BrC may be attributed to low volatility oxygenated organic compounds, which has also been detected in heated (300 °C) particles (Poulain et al., 2014). Therefore, the estimated $\sigma_{abs,BrC}/\sigma_{abs,370nm}$ based on Method II should suffer substantial error when there is high abundance of SOC.

From the co-located SPAMS, it was observed that detected number for internally mixed OC and sulfate (OC-sulfate) particles, which is frequently observed in the atmosphere of PRD region (Zhang et al., 2015), substantially increased during noon hours when aerosols were heated (Fig. S3). More efficient detection of these particles in this case is probably linked to increased absorption of ablation laser by heated OC-sulfate particles (Hatch et al., 2014). With strong absorbing EC cores, the increased absorption is therefore more likely attributed to the formation of absorptive species (i.e., BrC) in heated OC-sulfate particles. Together with significant correlation between the estimated $\sigma_{abs,BrC}/\sigma_{abs,370nm}$ and SOC and sulfate (Fig. 6), it is suspected that the formed BrC during heating measurements might be linked to organosulfate, which was ionized to fragments representative of OC and sulfate in the internally mixed OC and sulfate particles (Hatch et al., 2011). Light absorption at shorter wavelength had been observed for organosulfate (Song et al., 2013). Although secondary organic aerosol (SOA) produced by photo-chemical ageing may contribute to BrC (Lambe et al., 2013; Saleh et al., 2013), our results indicate primary emission plays a dominant role. As discussed above, significant correlations between the estimated $\sigma_{abs,BrC}$ and BC, and potassium were observed. Furthermore, there is no correlation ($r^2 < 0.01$) between the estimated $\sigma_{abs,BrC}$ by our developed method and SOC (Fig. S4). As noted by Lambe et al. (2013), the extent of absorption by SOA is linked with the magnitude dependent on both precursor type and oxidation level.

4 Conclusions

The paper provides an improved AAE-based method to quantitative estimate the light absorption by BrC in real-time based on multi-wavelength light absorption measurements. The analysis shows that the wavelength dependence of BC light absorption can be better approximated over the higher (880–950 nm) wavelengths. Based on simultaneous measurements of σ_{abs} for both ambient and heated aerosols, $AAE_{880–950}$ was found to show negligible response to the presence of BrC and thus the application of AAE = $AAE_{880–950}$ (0.70 ± 0.07) for "pure" BC, instead of AAE = 1, should be more acceptable in the estimation of light absorption by BrC in the PRD region. However, the detected AAE value around 0.7 for this work could not represent all kinds of situations, in particular, when BrC absorption over longer wavelength is non-negligible. BrC was estimated to contribute to 37.4% of light absorption at 370 nm by the developed method, and it was largely attributed to primary emissions. The contribution is > 20% on average larger than that estimated by assuming AAE to be one. The results also suggest that the estimated contribution of BrC to total light absorption at 370 nm based on light absorption enhancement method might suffer potential error when there are high loading of SOA. It might serve as evidence for the production of BrC when aerosols were heated, which was neglected in previous studies.

Acknowledgements

This work was supported by the National Nature Science Foundation of China (No. 41775124), and the State Key Laboratory of Organic Geochemistry (SKLOGA201603A), and Guangdong Provincial Key Laboratory of Environmental Protection and Resources Utilization (2014B030301060). The authors would also like to thank all participants for the sampling at the Guangdong Atmospheric Supersite.

References

Ajtai, T., Filep, A., Utry, N., Schnaiter, M., Linke, C., Bozoki, Z., Szabo, G., Leisner, T. (2011). Inter-comparison of optical absorption coefficients of atmospheric aerosols determined by a multi-wavelength photoacoustic spectrometer and an Aethalometer under sub-urban wintry conditions. *J. Aerosol Sci.* 42: 859-866.

Alexander, D. T. L., Crozier, P. A., Anderson, J. R. (2008). Brown carbon spheres in East Asian outflow and their optical properties. *Science* 321: 833-836.

Andreae, M. O. and Gelencser, A. (2006). Black carbon or brown carbon? The nature of light-absorbing carbonaceous aerosols. *Atmos. Chem. Phys.* 6: 3131-3148.

Arnott, W. P., Hamasha, K., Moosmuller, H., Sheridan, P. J., Ogren, J. A. (2005). Towards aerosol light-absorption measurements with a 7-wavelength Aethalometer: Evaluation with a photoacoustic instrument and 3-wavelength nephelometer. *Aerosol Sci. Tech.* 39: 17-29.

Bahadur, R., Praveen, P. S., Xu, Y. Y., Ramanathan, V. (2012). Solar absorption by elemental and brown carbon determined from spectral observations. *Proc. Natl. Acad. Sci. USA* 109: 17366-17371.

Bergstrom, R. W., Pilewskie, P., Russell, P. B., Redemann, J., Bond, T. C., Quinn, P. K., Sierau, B. (2007). Spectral absorption properties of atmospheric aerosols. *Atmos. Chem. Phys.* 7: 5937-5943.

Bi, X. H., Dai, S. H., Zhang, G. H., Qiu, N., Li, M., Wang, X. M., Chen, D. H., Peng, P. A., Sheng, G. Y., Fu, J. M., Zhou, Z. (2015). Real-time and single-particle volatility of elemental carbon-containing particles in the urban area of Pearl River Delta region, China. *Atmos. Environ.* 118: 194-202.

Bond, T. C. and Bergstrom, R. W. (2006). Light absorption by carbonaceous particles: An investigative review. *Aerosol Sci. Tech.* 40: 27-67.

Cappa, C. D., Onasch, T. B., Massoli, P., Worsnop, D. R., Bates, T. S., Cross, E. S., Davidovits, P., Hakala, J., Hayden, K. L., Jobson, B. T., Kolesar, K. R., Lack, D. A., Lerner, B. M., Li, S. M., Mellon, D., Nuaaman, I., Olfert, J. S., Petaja, T., Quinn, P. K., Song, C., Subramanian, R., Williams, E. J., Zaveri, R. A. (2012). Radiative Absorption Enhancements Due to the Mixing State of Atmospheric Black Carbon. *Science* 337: 1078-1081.

Chen, X. J., Lai, S. C., Gao, Y., Zhang, Y. Y., Zhao, Y., Chen, D. H., Zheng, J. Y., Zhong, L. J., Lee, S. C., Chen, B. (2016). Reconstructed Light Extinction Coefficients of Fine Particulate Matter in Rural Guangzhou, Southern China. *Aerosol Air Qual. Res.* 16: 1981-1990.

Cheng, Y., He, K. B., Zheng, M., Duan, F. K., Du, Z. Y., Ma, Y. L., Tan, J. H., Yang, F. M., Liu, J. M., Zhang, X. L., Weber, R. J., Bergin, M. H., Russell, A. G. (2011). Mass absorption efficiency of elemental carbon and water-soluble organic carbon in Beijing, China. *Atmos. Chem. Phys.* 11: 11497-11510.

Cheng, Y. F., Wiedensohler, A., Eichler, H., Su, H., Gnauk, T., Brüggemann, E., Herrmann, H., Heintzenberg, J., Slanina, J., Tuch, T., Hu, M., Zhang, Y. H. (2008). Aerosol optical properties and related chemical apportionment at Xinken in Pearl River Delta of China. *Atmos. Environ.* 42: 6351-6372.

Corr, C. A., Hall, S. R., Ullmann, K., Anderson, B. E., Beyersdorf, A. J., Thornhill, K. L., Cubison, M. J., Jimenez, J. L., Wisthaler, A., Dibb, J. E. (2012). Spectral absorption of biomass burning aerosol determined from retrieved single scattering albedo during ARCTAS. *Atmos. Chem. Phys.* 12: 10505-10518.

Drinovec, L., Močnik, G., Zotter, P., Prévôt, A. S. H., Ruckstuhl, C., Coz, E., Rupakheti, M., Sciare, J., Müller, T., Wiedensohler, A., Hansen, A. D. A. (2015). The "dual-spot" Aethalometer: an improved measurement of aerosol black carbon with real-time loading compensation. *Atmos. Meas. Tech.* 8: 1965-1979.

Favez, O., Alfaro, S. C., Sciare, J., Cachier, H., Abdelwahab, M. M. (2009). Ambient measurements of light-absorption by agricultural waste burning organic aerosols. *J. Aerosol Sci.* 40: 613-620.

Feng, Y., Ramanathan, V., Kotamarthi, V. R. (2013). Brown carbon: a significant atmospheric absorber of solar radiation? *Atmos. Chem. Phys.* 13: 8607-8621.

Guo, X. S., Nakayama, T., Yamada, H., Inomata, S., Tonokura, K., Matsumi, Y. (2014). Measurement of the light absorbing properties of diesel exhaust particles using a three-wavelength photoacoustic spectrometer. *Atmos. Environ.* 94: 428-437.

Gyawali, M., Arnott, W. P., Lewis, K., Moosmuller, H. (2009). In situ aerosol optics in Reno, NV, USA during and after the summer 2008 California wildfires and the influence of absorbing and non-absorbing organic coatings on spectral light absorption. *Atmos. Chem. Phys.* 9: 8007-8015.

Harrison, R. M., Beddows, D. C. S., Hu, L., Yin, J. (2012). Comparison of methods for evaluation of wood smoke and estimation of UK ambient concentrations. *Atmos. Chem. Phys.* 12: 8271-8283.

Hatch, L. E., Creamean, J. M., Ault, A. P., Surratt, J. D., Chan, M. N., Seinfeld, J. H., Edgerton, E. S., Su, Y., Prather, K. A. (2011). Measurements of Isoprene-Derived Organosulfates in Ambient Aerosols by Aerosol Time-of-Flight Mass Spectrometry - Part 1: Single Particle Atmospheric Observations in Atlanta. *Environ. Sci. Technol.* 45: 5105-5111.

Hatch, L. E., Pratt, K. A., Huffman, J. A., Jimenez, J. L., Prather, K. A. (2014). Impacts of Aerosol Aging on Laser Desorption/Ionization in Single-Particle Mass Spectrometers. *Aerosol Sci. Tech.*: 1050-1058.

Hsiao, T. C., Ye, W. C., Wang, S. H., Tsay, S. C., Chen, W. N., Lin, N. H., Lee, C. T., Hung, H. M., Chuang, M. T., Chantara, S. (2016). Investigation of the CCN Activity, BC and UVBC Mass Concentrations of Biomass Burning Aerosols during the 2013 BASELInE Campaign. *Aerosol Air Qual. Res.* 16: 2742-2756.

Huang, X. F., Gao, R. S., Schwarz, J. P., He, L. Y., Fahey, D. W., Watts, L. A., McComiskey, A., Cooper, O. R., Sun, T. L., Zeng, L. W., Hu, M., Zhang, Y. H. (2011). Black carbon measurements in the Pearl River Delta region of China. *J. Geophys. Res.* 116: 445-451.

Kirchstetter, T. W., Novakov, T., Hobbs, P. V. (2004). Evidence that the spectral dependence of light absorption by aerosols is affected by organic carbon. *J. Geophys. Res.-Atmos.* 109: 21208.

Kirchstetter, T. W. and Thatcher, T. L. (2012). Contribution of organic carbon to wood smoke particulate matter absorption of solar radiation. *Atmos. Chem. Phys.* 12: 6067-6072.

Lack, D. A. and Cappa, C. D. (2010). Impact of brown and clear carbon on light absorption enhancement, single scatter albedo and absorption wavelength dependence of black carbon. *Atmos. Chem. Phys.* 10: 4207-4220.

Lack, D. A., Bahreni, R., Langridge, J. M., Gilman, J. B., Middlebrook, A. M. (2013). Brown carbon absorption linked to organic mass tracers in biomass burning particles. *Atmos. Chem. Phys.* 13: 2415-2422.

Lack, D. A. and Langridge, J. M. (2013). On the attribution of black and brown carbon light absorption using the Angstrom exponent. *Atmos. Chem. Phys.* 13: 10535-10543.

Lambe, A. T., Cappa, C. D., Massoli, P., Onasch, T. B., Forestieri, S. D., Martin, A. T., Cummings, M. J., Croasdale, D. R., Brune, W. H., Worsnop, D. R., Davidovits, P. (2013). Relationship between Oxidation Level and Optical Properties of Secondary Organic Aerosol. *Environ. Sci. Technol.* 47: 6349-6357.

Laskin, A., Laskin, J., Nizkorodov, S. A. (2015). Chemistry of Atmospheric Brown Carbon. *Chem. Rev.* 115: 4335-4382.

Li, L., Huang, Z. X., Dong, J. G., Li, M., Gao, W., Nian, H. Q., Fu, Z., Zhang, G. H., Bi, X. H., Cheng, P., Zhou, Z. (2011). Real time bipolar time-of-flight mass spectrometer for analyzing single aerosol particles. *Intl. J. Mass. Spectrom.* 303: 118-124.

Lin, C. C., Yang, L. S., Cheng, Y. H. (2016). Ambient PM2.5, Black Carbon, and Particle Size-Resolved Number Concentrations and the Angstrom Exponent Value of Aerosols during the Firework Display at the Lantern Festival in Southern Taiwan. *Aerosol Air Qual. Res.* 16: 373-387.

Liu, J., Scheuer, E., Dibb, J., Ziemba, L. D., Thornhill, K. L., Anderson, B. E., Wisthaler, A., Mikoviny, T., Devi, J. J., Bergin, M., Weber, R. J. (2014). Brown carbon in the continental troposphere. *Geophys. Res. Lett.* 41: 2191-2195.

Liu, J., Scheuer, E., Dibb, J., Diskin, G. S., Ziemba, L. D., Thornhill, K. L., Anderson, B. E., Wisthaler, A., Mikoviny, T., Devi, J. J., Bergin, M., Perring, A. E., Markovic, M. Z., Schwarz, J. P., Campuzano-Jost, P., Day, D. A., Jimenez, J. L., Weber, R. J. (2015). Brown carbon aerosol in the North American continental troposphere: sources, abundance, and radiative forcing. *Atmos. Chem. Phys.* 15: 7841-7858.

McMeeking, G. R., Fortner, E., Onasch, T. B., Taylor, J. W., Flynn, M., Coe, H., Kreidenweis, S. M. (2014). Impacts of nonrefractory material on light absorption by aerosols emitted from biomass burning. *J. Geophys. Res.-Atmos.* 119: 12272-12286.

Mogo, S., Cachorro, V. E., de Frutos, A., Rodrigues, A. (2012). Absorption Angstrom exponents of aerosols and light absorbing carbon (LAC) obtained from in situ data in Covilha, central Portugal. *J. Environ. Monitor.* 14: 3174-3181.

Moosmüller, H., Chakrabarty, R. K., Arnott, W. P. (2009). Aerosol light absorption and its measurement: A review. *J. Quant. Spectrosc. Ra-diat. Transfer* 110: 844-878.

Moosmüller, H., Chakrabarty, R. K., Ehlers, K. M., Arnott, W. P. (2011). Absorption Ångström coefficient, brown carbon, and aerosols: basic concepts, bulk matter, and spherical particles. *Atmos. Chem. Phys.* 11: 1217-1225.

Nakayama, T., Ikeda, Y., Sawada, Y., Setoguchi, Y., Ogawa, S., Kawana, K., Mochida, M., Ikemori, F., Matsumoto, K., Matsumi, Y. (2014). Properties of light-absorbing aerosols in the Nagoya urban area, Japan, in August 2011 and January 2012: Contributions of brown carbon and lensing effect. *J. Geophys. Res.-Atmos.* 119: 12721-12739.

Pintér, M., Ajtai, T., Kiss-Albert, G., Kiss, D., Utry, N., Janovszky, P., Palásti, D., Smausz, T., Kohut, A., Hopp, B., Galbács, G., Kukovecz, Á., Kónya, Z., Szabó, G., Bozóki, Z. (2018). Thermo-optical properties of residential coals and combustion aerosols. *Atmos. Environ.* 178: 118-128.

Poulain, L., Birmili, W., Canonaco, F., Crippa, M., Wu, Z. J., Nordmann, S., Spindler, G., Prevot, A. S. H., Wiedensohler, A., Herrmann, H. (2014). Chemical mass balance of 300 degrees C non-volatile particles at the tropospheric research site Melpitz, Germany. *Atmos. Chem. Phys.* 14: 10145-10162.

Qin, Y. M., Tan, H. B., Li, Y. J., Schurman, M. I., Li, F., Canonaco, F., Prevot, A. S. H., Chan, C. K. (2017). Impacts of traffic emissions on atmospheric particulate nitrate and organics at a downwind site on the periphery of Guangzhou, China. *Atmos. Chem. Phys.* 17: 10245-10258.

Rathod, T., Sahu, S. K., Tiwari, M., Yousaf, A., Bhangare, R. C., Pandit, G. G. (2017). Light Absorbing Properties of Brown Carbon Generated from Pyrolytic Combustion of Household Biofuels. *Aerosol Air Qual. Res.* 17: 108-116.

Rumsey, I. C., Cowen, K. A., Walker, J. T., Kelly, T. J., Hanft, E. A., Mishoe, K., Rogers, C., Proost, R., Beachley, G. M., Lear, G., Frelink, T., Otjes, R. P. (2014). An assessment of the performance of the Monitor for AeRosols and GAses in ambient air (MARGA): a semi-continuous method for soluble compounds. *Atmos. Chem. Phys.* 14: 5639-5658.

Saleh, R., Hennigan, C. J., McMeeking, G. R., Chuang, W. K., Robinson, E. S., Coe, H., Donahue, N. M., Robinson, A. L. (2013). Absorptivity of brown carbon in fresh and photo-chemically aged biomass-burning emissions. *Atmos. Chem. Phys.* 13: 7683-7693.

Saleh, R., Robinson, E. S., Tkacik, D. S., Ahern, A. T., Liu, S., Aiken, A. C., Sullivan, R. C., Presto, A. A., Dubey, M. K., Yokelson, R. J., Donahue, N. M., Robinson, A. L. (2014). Brownness of organics in aerosols from biomass burning linked to their black carbon content. *Nature Geosci.* 7: 647-650.

Sandradewi, J., Prevot, A. S. H., Weingartner, E., Schmidhauser, R., Gysel, M., Baltensperger, U. (2008). A study of wood burning and traffic aerosols in an Alpine valley using a multi-wavelength Aethalometer. *Atmos. Environ.* 42: 101-112.

Shamjad, P. M., Tripathi, S. N., Pathak, R., Hallquist, M., Arola, A., Bergin, M. H. (2015). Contribution of Brown Carbon to Direct Radiative Forcing over the Indo-Gangetic Plain. *Environ. Sci. Technol.* 49: 10474-10481.

Shrestha, R., Kim, S. W., Yoon, S. C., Kim, J. H. (2014). Attribution of aerosol light absorption to black carbon and volatile aerosols. *Environ. Monit. Assess.* 186: 4743-4751.

Song, C., Gyawali, M., Zaveri, R. A., Shilling, J. E., Arnott, W. P. (2013). Light absorption by secondary organic aerosol from alpha-pinene: Effects of oxidants, seed aerosol acidity, and relative humidity. *J. Geophys. Res.-Atmos.* 118: 11741-11749.

Stevanovic, S., Miljevic, B., Madl, P., Clifford, S., Ristovski, Z. (2015). Characterisation of a Commercially Available Thermodenuder and Diffusion Drier for Ultrafine Particles Losses. *Aerosol Air Qual. Res.* 15: 357-+.

Utry, N., Ajtai, T., Filep, Á., Pintér, M., Török, Z., Bozóki, Z., Szabó, G. (2014). Correlations between absorption Angström exponent (AAE) of wintertime ambient urban aerosol and its physical and chemical properties. *Atmos. Environ.* 91: 52-59.

Villani, P., Picard, D., Marchand, N., Laj, P. (2007). Design and validation of a 6-volatility tandem differential mobility analyzer (VTDMA). *Aerosol Sci. Tech.* 41: 898-906.

Wu, Y. F., Yan, P., Tian, P., Tao, J., Li, L., Chen, J. M., Zhang, Y. M., Cao, N. W., Chen, C., Zhang, R. J. (2015). Spectral Light Absorption of Ambient Aerosols in Urban Beijing during Summer: An Intercomparison of Measurements from a Range of Instruments. *Aerosol Air Qual. Res.* 15: 1178-1187.

Yang, M., Howell, S. G., Zhuang, J., Huebert, B. J. (2009). Attribution of aerosol light absorption to black carbon, brown carbon, and dust in China - interpretations of atmospheric measurements during EAST-AIRE. *Atmos. Chem. Phys.* 9: 2035-2050.

Yuan, J. F., Huang, X. F., Cao, L. M., Cui, J., Zhu, Q., Huang, C. N., Lan, Z. J., He, L. Y. (2016). Light absorption of brown carbon aerosol in the PRD region of China. *Atmos. Chem. Phys.* 16: 1433-1443.

Zhang, G. H., Bi, X. H., Chan, L. Y., Wang, X. M., Sheng, G. Y., Fu, J. M. (2013a). Size-segregated chemical characteristics of aerosol during haze in an urban area of the Pearl River Delta region, China. *Urban Climate* 4: 74-84.

Zhang, G. H., Bi, X. H., He, J. J., Chen, D. H., Chan, L. Y., Xie, G. W., Wang, X. M., Sheng, G. Y., Fu, J. M., Zhou, Z. (2014). Variation of secondary coatings associated with elemental carbon by single particle analysis. *Atmos. Environ.* 92: 162-170.

Zhang, G. H., Han, B. X., Bi, X. H., Dai, S. H., Huang, W., Chen, D. H., Wang, X. M., Sheng, G. Y., Fu, J. M., Zhou, Z. (2015). Characteristics of individual particles in the atmosphere of Guangzhou by single particle mass spectrometry. *Atmos. Res.* 153: 286-295.

Zhang, X., Lin, Y.-H., Surratt, J. D., Weber, R. J. (2013b). Sources, Composition and Absorption Ångström Exponent of Light-absorbing Organic Components in Aerosol Extracts from the Los Angeles Basin. *Environ. Sci. Technol.* 47: 3685-3693.

Zhu, J., Crozier, P. A., Anderson, J. R. (2013). Characterization of light-absorbing carbon particles at three altitudes in East Asian outflow by transmission electron microscopy. *Atmos. Chem. Phys.* 13: 6359-6371.

List of figure captions

Fig. 1. An illustration of the method to estimate the contribution of light absorption from BrC, based on the assumption of AAE = 1 for Method I, and AAE = $AAE_{880–950}$ for our developed method.

Fig. 2. (a) Comparison of AAE at the wavelength of 370–520, 880–950, and 370–950 nm, and diurnal variations of AAE at the wavelength of (b) 370–520 nm and (c) 880–950 nm, for aerosols before and after heated, respectively.

Fig. 3. (a) Temporal profile of $\sigma_{abs,BrC}$ and the concentration of potassium, (b) correlation analysis of $\sigma_{abs,BrC}$ and the concentration of BC, and (c) the histogram summarizing of the $\sigma_{abs,BrC}/\sigma_{abs,370nm}$ over this study.

Fig. 4. Comparison of $\sigma_{abs,BrC}/\sigma_{abs,370nm}$ estimated by our developed method and Methods I based on AAE = 1.

Fig. 5. Comparisons of (a) diurnal variations and (b) hourly averaged $\sigma_{abs,BrC}/\sigma_{abs,370nm}$ estimated by Methods II and our developed method.

Fig. 6. Correlation plots between the $\sigma_{abs,BrC}/\sigma_{abs,370nm}$ estimated by Method II and the concentrations of O_3, SOC, OC and sulfate.

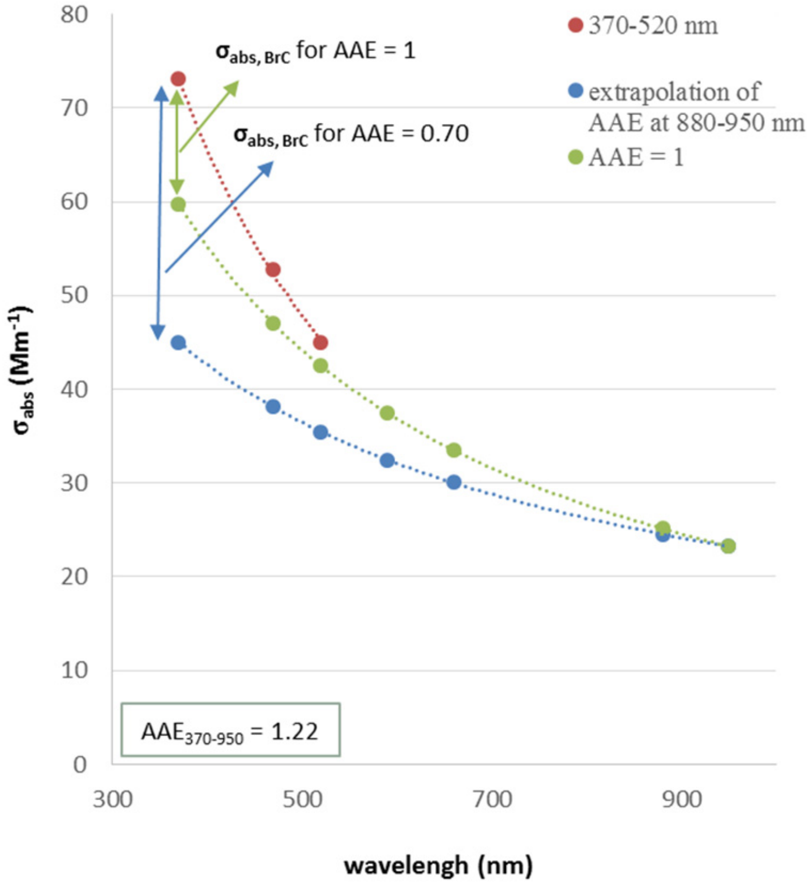

370-520 nm
extrapolation of AAE at 880-950 nm
AAE = 1
σabs, BrC for AAE = 1
σabs, BrC for AAE = 0.70
AAE370-950 = 1.22
σabs (Mm-1)
wavelengh (nm)
0
10
20
30
40
50
60
70
80
300
500
700
900

Fig. 1.

545
546

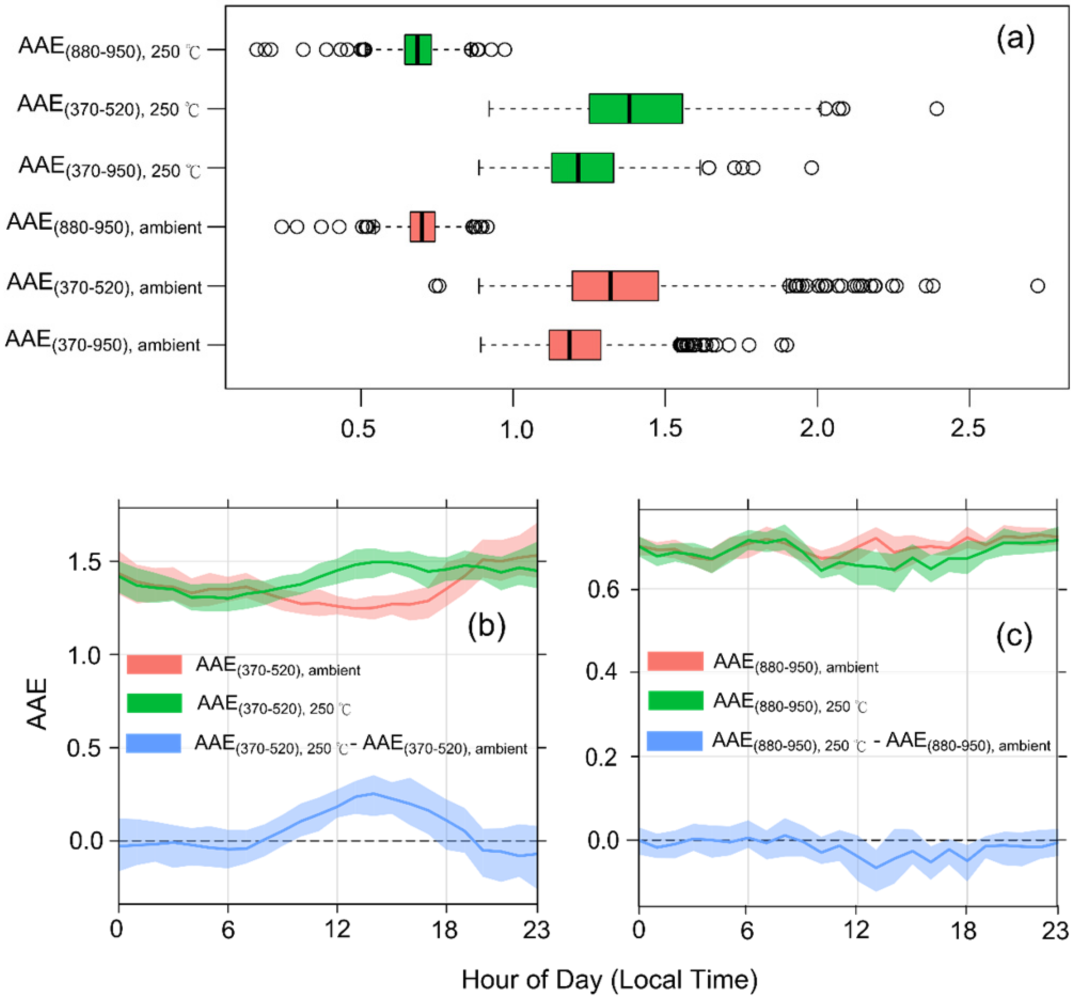

547 Fig. 2.

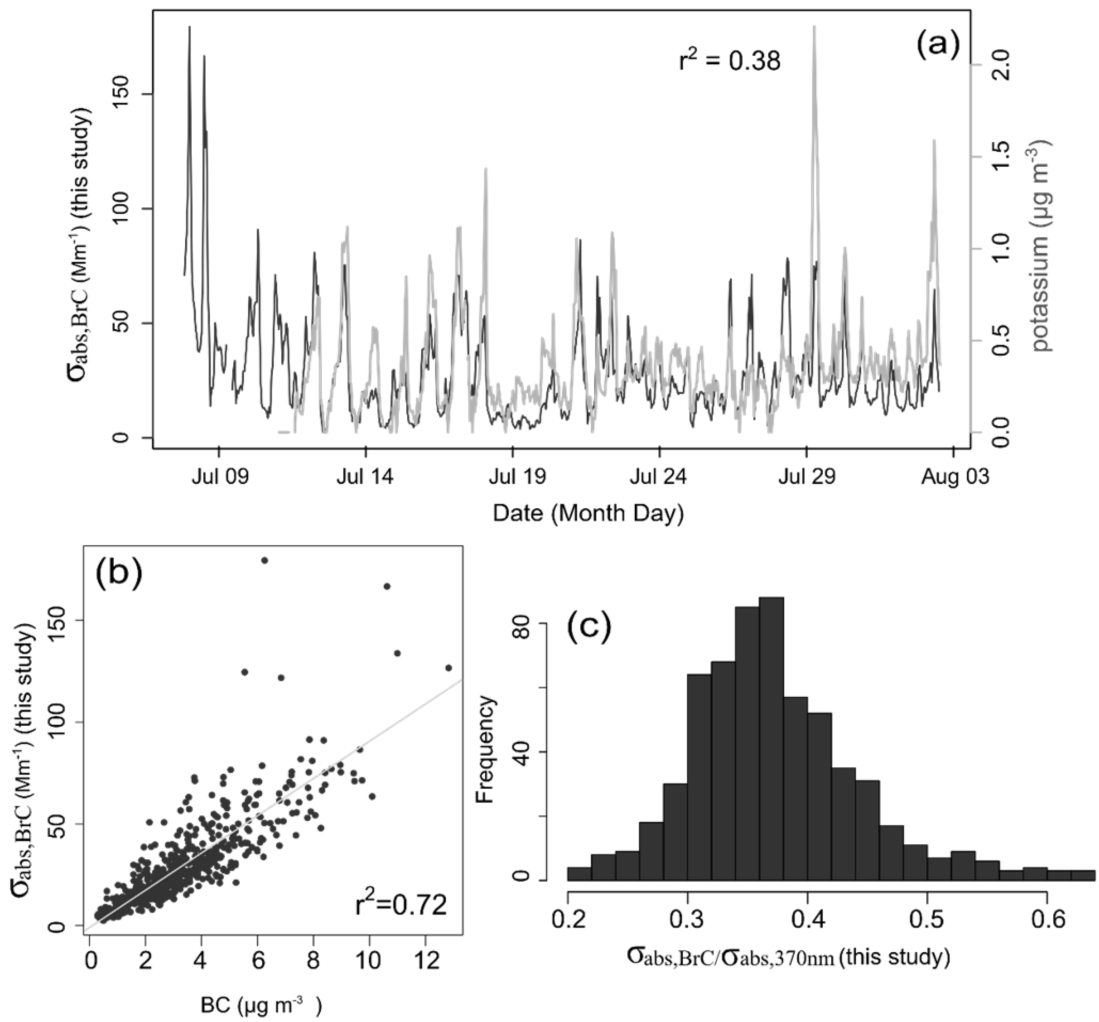

(a)
r² = 0.38
σabs,BrC (Mm⁻¹) (this study)
potassium (μg m⁻³)
Jul 09
Jul 14
Jul 19
Jul 24
Jul 29
Aug 03
Date (Month Day)
(b)
σabs,BrC (Mm⁻¹) (this study)
r²=0.72
BC (μg m⁻³)
(c)
Frequency
σabs,BrC/σabs,370nm (this study)

Fig. 3.

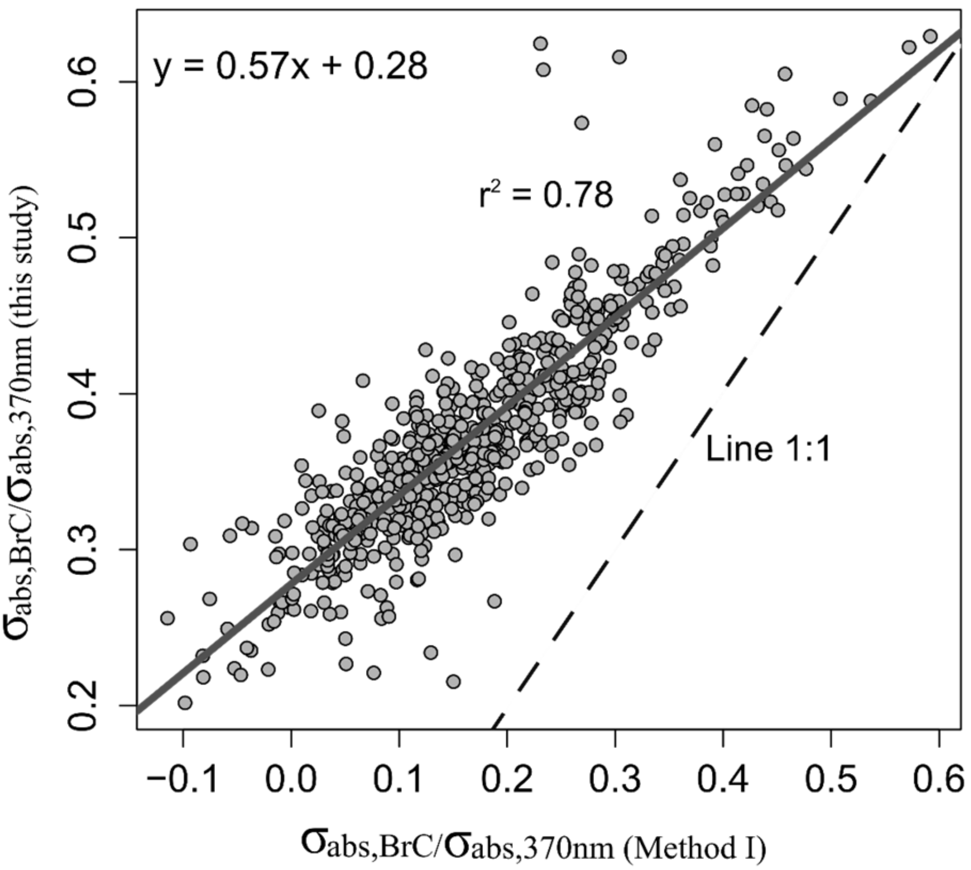
y = 0.57x + 0.28
r² = 0.78
Line 1:1
0.2
0.3
0.4
0.5
0.6
−0.1
0.0
0.1
0.2
0.3
0.4
0.5
0.6
σabs,BrC/σabs,370nm (this study)
σabs,BrC/σabs,370nm (Method I)

Fig. 4.

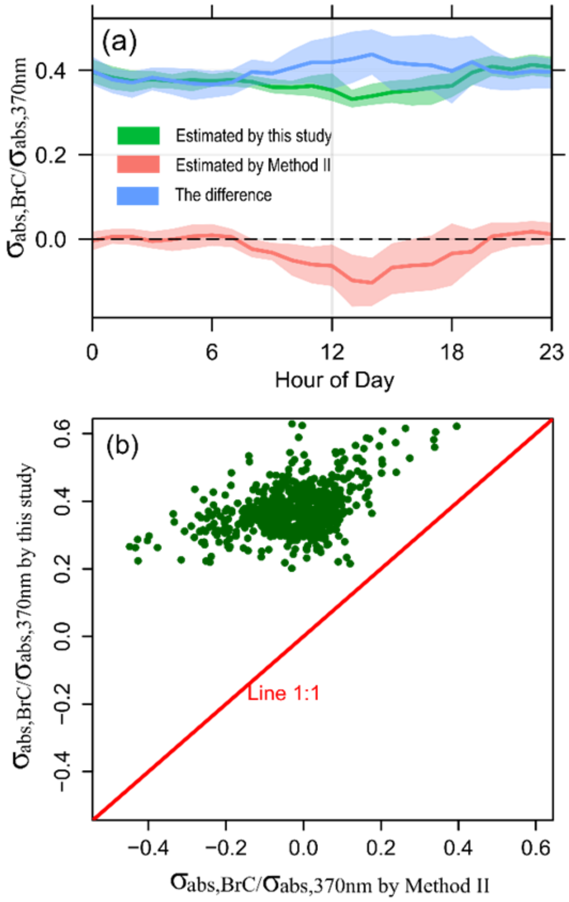

554

555

556 Fig. 5.

557

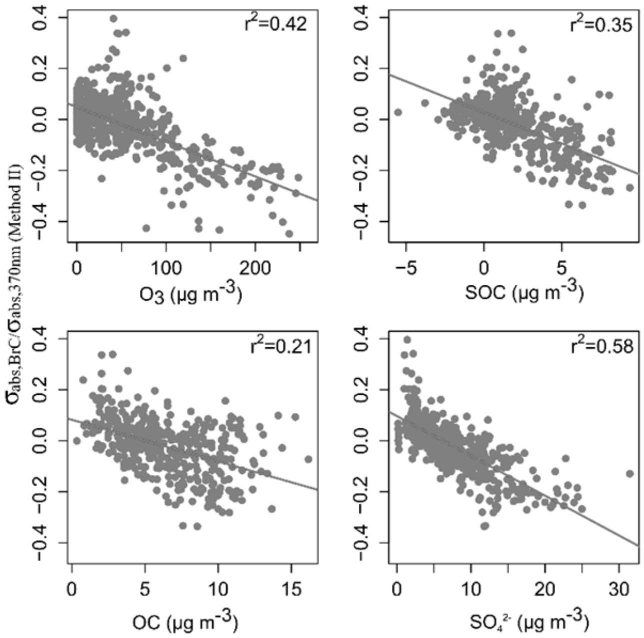
r^2=0.42
r^2=0.35
r^2=0.21
r^2=0.58
σabs,BrC/σabs,370nm (Method II)
O3 (μg m^{-3})
SOC (μg m^{-3})
OC (μg m^{-3})
SO$_4^{2-}$ (μg m^{-3})

Fig. 6.